RESEARCH ARTICLE

RGD-peptide lunasin inhibits Akt-mediated NF-κB activation in human macrophages through interaction with the αVβ3 integrin

Anthony Cam and Elvira Gonzalez de Mejia

Department of Food Science and Human Nutrition, University of Illinois at Urbana-Champaign, IL, USA

Received: May 20, 2012
Revised: June 14, 2012
Accepted: June 19, 2012

Scope: Cardiovascular disease is the leading cause of mortality in the United States and regulation of aberrant macrophage activity under inflammatory conditions is critical for its prevention. The objective was to determine the effect of lunasin on the inhibition of Akt-mediated activation of nuclear factor-kappa B (NF-κB)-dependent markers of inflammation and to characterize the physical interaction of lunasin with the αVβ3 integrin receptor in lipopolysaccharide (LPS)-induced human THP-1 macrophages.
Methods and results: The effect of lunasin was evaluated in vitro in LPS-induced THP-1 human macrophages using immunoassays, co-immunoprecipitation (Co-IP), and fluorescence confocal microscopy. Lunasin (50 μM) reduced cyclooxygenase-2, inducible nitric oxide synthase, and NO levels by 57.9, 64.5, and 76.2%, respectively, and inhibited the activation of phosphorylated Akt and NF-κB p65 by 59.5 and 74.5%, respectively. Lunasin (50 μM) reduced exogenous release of prostaglandin E_2 and tumor necrosis factor-α by 92.5 and 94.9%, respectively. Vitronectin (10 μg/mL), an integrin ligand, increased expression of proinflammatory markers, whereas lunasin (50 μM) attenuated them. Co-IP of lunasin-treated cells confirmed direct interaction with αVβ3 integrin and LC/MS/MS verified its identity. Lunasin was detected within intracellular vesicles and reduced total αVβ3 intensity as observed by fluorescence microscopy.
Conclusion: Lunasin inhibited αVβ3 integrin-mediated proinflammatory markers and down-regulated Akt-mediated NF-κB pathways through interaction with αVβ3 integrin.

Keywords:
Atherosclerosis / Cardiovascular disease / Inflammation / Integrin / RGD Peptide

1 Introduction

Cardiovascular disease (CVD) is the leading cause of death in the United States (US) [1]. The estimated cost for treatment of CVD in the US is expected to increase from $273 billion to $818 billion/year between 2010 and 2030 [2, 3]. Diet has a significant impact on hypertension, obesity, and diabetes, which are major risk factors for the development of CVD, specifically atherosclerosis. Initiation and progression of atherosclerosis is influenced extensively by inflammation [4]. Peptides derived from soybean have been shown to elicit potent anti-inflammatory effects [5–7].

Soybean is a high-protein, nutrient dense food that possesses biologically active peptides such as lunasin. The Food and Drug Administration approved the claim that 25 g of soy protein a day, as part of a diet low in saturated fat and cholesterol, may reduce the risk of heart disease [8]. A meta-analysis of randomized, controlled studies on the effect of soy protein consumption on risk factors for CVD found a median intake of 30 g/day significantly improved serum lipoprotein levels [9]. Although chronic inflammation has been implicated as a major contributor to the progression of atherosclerosis [10], further research into the molecular effect of soy protein would provide potential implications for the prevention of CVD.

Lunasin, a 43–amino-acid bioactive peptide derived from soybean, contains a unique Arg-Gly-Asp (RGD) cell adhesion motif and polyaspartic acid tail [11]. The bioavailability of lunasin in humans was demonstrated by its presence in plasma after consumption of soy protein foods [12]. Lunasin inhibits

Correspondence: Dr. Elvira Gonzalez de Mejia, 228 ERML, MC-051, 1201 West Gregory Drive, Urbana, IL 61801, USA
E-mail: edemejia@illinois.edu
Fax: +1-217-265–0925

Abbreviations: **Co-IP**, co-immunoprecipitation; **COX-2**, cyclooxygenase-2; **CVD**, cardiovascular disease; **iNOS**, inducible nitric oxide synthase; **NFκB**, nuclear factor-kappa B; **PGE2**, prostaglandin E2; **PMA**, phorbol 12-myristate 13-acetate; **RGD**, arginine-glycine-aspartic acid; **TNF-α**, tumor necrosis factor α

inflammation though suppression of nuclear factor-kappa B (NF-κB) in murine macrophages [6]. However, the molecular mechanisms of these effects and its potential significance in the pathogenesis of atherosclerosis have not been studied in human macrophages.

Integrins are ubiquitous receptors that act as a signaling medium between the cytoskeleton and extracellular matrix and play a significant role in regulatory processes such as gene expression, proliferation, migration, and survival [13–15]. Peptides containing RGD motifs bind integrins with high specificity, leading to antiangiogenic and anti-inflammatory effects [16–18]. Under homeostatic conditions, macrophages are important elements of the immune response, and functions include phagocytosis of pathogens and release of signaling cytokines. However, chronic states of inflammation induce aggregation of macrophages with high expression of αVβ3 integrins to atherosclerotic lesions [19, 20]. A synthetic cyclic RGD peptide abolished the release of inflammatory cytokines from human macrophages with high expression of αVβ3 integrin [21]. Further, synthetic monoclonal antibodies directed to block αVβ3 integrin ligand activation inhibited the development of atherosclerotic lesions in diabetic pigs with vascular tissue disease [22, 23].

The activation of αVβ3 integrin has been associated with inflammatory cascades involved in the Akt signaling pathway, an important mediator for cell growth, migration and survival [24]. NF-κB is a family of transcription factors that can be regulated by PI3K/Akt [24] and induce the expression of genes involved in important immune and inflammatory responses.

The objective of this work was to determine the effect of lunasin on the inhibition of Akt-mediated activation of NF-κB-dependent markers of inflammation and characterize the physical interaction of lunasin with the αVβ3 integrin receptor in LPS-induced human THP-1 macrophages.

2 Materials and methods

2.1 Materials

Human acute monocytic leukemia cell line (THP-1) and Roswell Park Memorial Institute-1640 media (RPMI-1640) were purchased from American Type Culture Collection (Manassas, VA, USA). Fetal bovine serum (FBS) was purchased from Thermo Scientific (Logan, UT, USA). Streptomycin/penicillin and sodium pyruvate were purchased from Cellgro (Manassas, VA, USA). LPS from *Escherichia coli* O55:B5, echistatin, and phorbol 12-myristate 13-acetate (PMA) were purchased from Sigma-Aldrich (St. Louis, MO, USA). Human recombinant vitronectin was purchased from LD Biopharma (San Diego, CA, USA). Mouse Ab to phospho-Akt (p-Akt), phospho-p65 (p-p65), and αVβ3 integrin; Protein A/G PLUS-Agarose Immunoprecipitation Reagent, RIPA buffer, and normal mouse IgG were from Santa Cruz Biotechnology (Santa Cruz, CA, USA). Alexa Fluor 568 Goat Anti-Rabbit IgG, Alexa Fluor 488 Goat Anti-Mouse IgG, ImageiT FX signal Enhancer, ProLong Gold antifade reagent with DAPI, and phenol red-free RPMI-1640 were purchased from Life Technologies (Carlsbad, CA, USA). Paraformaldehyde (16%) aqueous solution was purchased from Electron Microscopy Sciences (Hatfield, PA, USA). IbiTreat μ-Slide eight-well microscopy chambers were purchased from ibidi (Munich, Germany).

Lunasin (>95%) was purified from defatted soybean flour using a modified protocol [25]. Briefly, defatted soy flour (Archer Daniels Midland, Decatur, IL, USA) and deionized water (1:5) were stirred for 72 h at 4°C, and centrifuged at 12 000 × *g* for 10 min. The supernatant was collected and filtered with cheesecloth for anion-exchange chromatography. Fractions with the highest concentration of lunasin were pooled and salts were removed by ultrafiltration (1 kDa) (Millipore, Billerica, MA, USA) at 4°C using 20 psi helium gas until the retentate was 10% of the original volume. Protein was determined by DC Protein Assay (Biorad, Hercules, CA, USA). The retentate was diluted to 1 mg/mL with deionized water and loaded into 10 kDa ultracentrifugal filter units (Millipore, Billerica, MA, USA) and centrifuged at 5000 × *g* for 45 min at 25°C. The filtrate was pooled together and subjected to an additional round of ultracentrifugation to remove any remaining contaminant proteins. The purity and identity of lunasin was verified with ELISA, gel electrophoresis and Western blot. Lunasin was freeze-dried and stored at −20°C.

2.2 Cell Culture

2.2.1 Differentiation of THP-1 monocytes

THP-1 monocytic cell line was cultured in RPMI-1640 growth medium, 1% penicillin/streptomycin and 10% fetal bovine serum and incubated at 37°C in 5% CO_2/95% air. Monocytes were differentiated into macrophages in 48 h by addition of 100 nM PMA as previously described [19]. Macrophage differentiation was determined by cell morphology and total adhesion to the plate.

2.2.2 Cell proliferation

Cell proliferation was performed with the CellTiter 96 Aqueous One Solution Proliferation assay (Promega Corporation, Madison, WI, USA). Briefly, 2×10^4 cells/well were seeded in a 96-well plate and volume adjusted to 200 μL with growth medium. Differentiated macrophages were washed three times with fresh growth medium and treated with lunasin (10, 25, 50, and 100 μM) for 24 h. Medium was removed and 100 μL fresh growth medium and 20 μL MTS/PES were added to each well. The plate was incubated for 2 h at 37°C in 5% CO_2/95% air and absorbance read at 515 nm using an Ultra Microplate Reader (Bio-Tek Instruments, Winooski, VT, USA). Viable cells (%) were calculated with respect to cells treated with PBS control.

2.2.3 Treatments

Cells were differentiated (1×10^6 cells/well) in six-well culture plates and treated: lunasin pretreatment (10, 25, or 50 μM) or PBS for 2 h followed by LPS (1 μg/mL); or pretreatment with lunasin (50 or 100 μM) or PBS for 2 h followed by the addition of human vitronectin (10 μg/mL) alone or combined with LPS (1 μg/mL) for 24 h. After treatment, the spent medium was analyzed for nitric oxide (NO), prostaglandin E_2 (PGE_2), and tumor necrosis factor-α (TNF-α). Whole cell lysates were used to quantify the effect of lunasin on cyclooxygenase-2 (COX-2); inducible nitric oxide synthase (iNOX), nuclear factor-kappa B (NFκ B) p-p65, and p-Akt. Each treatment was performed in triplicate to confirm reproducibility.

2.3 Nitric oxide (NO)

Nitrite was measured by Griess reaction [26]. Briefly, 100 μL of the spent medium were plated in 96-well plate and an equal amount of Griess reagent (1% sulfanilamide and 0.1% *N*-1-(naphthyl)ethylenediamine-diHCl in 2.5% H_3PO_4) added, incubated for 5 min at 25°C, and absorbance measured at 550 nm using an Ultra Microplate Reader (Bio-Tek Instruments, Winooski, VT, USA). NO was calculated using sodium nitrite standard curve ($y = 3.60x + 75.80$, $R^2 = 0.99$).

2.4 PGE_2

PGE_2 was measured using a PGE_2 EIA monoclonal assay (Cayman Chemical, Ann Arbor, MI, USA). Briefly, 50 μL of diluted spent medium (1:5) was plated in 96-well goat anti-mouse IgG coated plate and incubated for 18 h at 4°C; the plate was washed and color developed by 200 μL of Ellman's reagent, gently shaking the plate (60–120 min) in the dark, and read at 405 nm using an Ultra Microplate Reader. PGE_2 calculated by standard curve ($y = -2.45x + 3.48$, $R^2 = 0.99$).

2.5 TNF-α

TNF-α was measured using TNF-α human ELISA (Abcam, Cambridge, MA, USA). Briefly, 100 μL of diluted spent medium (1:10) was plated in a 96-well plate precoated with a TNF-α mAb. Biotin-conjugated TNF-α mAb (50 μL) was added and the plate incubated for 3 h at 25°C. The plate was washed three times and 100 μL streptavidin-HP were added to all wells and incubated for 30 min. Following an additional wash, 100 μL TMB substrate were added and incubated for 10–15 min at 25°C in the dark. The reaction was stopped with 100 μL H_2SO_4 and read at 450 nm using an Ultra Microplate Reader. TNF-α concentration was calculated by TNF-α standard curve ($y = 1.60x + 71.70$, $R^2 = 0.98$).

2.6 Western blot analysis of iNOS, COX-2, p-p65, and p-Akt

Lunasin-treated cells were washed once with ice-cold RPMI-1640 and twice with ice-cold PBS before addition of 200 μL of lysing buffer (Laemmli buffer with 5% β-mercaptoethanol). After lysis, the lysates were sonicated and boiled for 5 min and protein was determined by RC-DC Protein Assay (Bio-rad) using BSA standard curve. Gel electrophoresis was performed by loading 20 μg protein per well in 4–20% Tris-HCl gels (BioRad). The separated proteins were transferred onto PVDF membranes and blocked with 5% BSA in 0.1% TBST for 1 h at 4°C. The membrane was washed with 0.1% TBST (five times, 5 min each) and incubated with mouse monoclonal antibodies (1:500) at 4°C overnight. Membranes were washed again and incubated with antimouse IgG horseradish peroxidase-conjugated secondary antibody (1:2500) for 1 h at 25°C. After washing with 0.1% TBST (five times, 5 min each), the expression of the proteins of interest was visualized using chemiluminescent reagent (GE Healthcare, Waukesha, WI, USA). Membrane picture was taken with a Kodak Image Station 440 CF (Eastman Kodak Company, Rochester, NY, USA).

2.7 Co-immunoprecipitation (Co-IP) of lunasin-αVβ3 integrin complex

Macrophages were differentiated at a density of 3×10^6 in 25 cm^2 flasks. After washing three times with fresh medium, one flask was treated with 10 μM lunasin for 24 h while another flask was left untreated as control. Cells were washed once with ice-cold RPMI-1640 and twice with PBS, and lysed with RIPA buffer (Santa Cruz Biotechnology). Lysates (1 mg protein) were placed in microcentrifuge tubes and 6 μg IgG_1 of αVβ3 integrin mAb was added. Cell lysates added with 1 μg normal IgG served as the control. Incubation with primary antibody was carried out for 8 h at 4°C. After, 60 μL of resuspended Protein A/G PlusAgarose beads (Santa Cruz Biotechnology) were added and placed in an end-over-end rotator mixer and incubated overnight at 4°C. Immunoprecipitates were collected, washed four times with RIPA buffer and eluted (Santa Cruz Biotechnology Inc.). Analysis of interaction between lunasin and αVβ3 integrin was performed using immunoblotting technique as described above. Three independent replicates were performed.

2.8 LC/MS/MS of Co-IP lunasin

MS analysis was conducted at the Protein Sciences Facility, Carver Biotechnology Center (University of Illinois, Urbana, IL, USA) using a Waters Q-ToF API-US mass spectrometer. The protein band in-gel slice of the lunasin Co-IP pull-down was crushed, destained, and dehydrated in 50% ACN containing 25 mM ammonium acetate. The protein was digested with proteomics grade trypsin

(G-Biosciences, St. Louis, MO, USA) in a CEM Discover Microwave Reactor (Mathews, NC, USA) for 15 min at 55°C at 50 Watts; extracted three times using 50% ACN containing 5% formic acid, pooled, and dried using a Speedvac (Thermo Scientific, Rockford, IL, USA). Peptides were suspended in 13 μL of 5% ACN containing 0.1% formic acid, and 10 μL injected for LC-MS. HPLC for the trypsin digested peptides was performed with a Waters nanoAcquity UPLC using a Waters Atlantis dC18 nanoAcquity column (3 μm beads, 75 μm inner diameter × 150 mm length), solvents (A) water containing 0.1% formic acid and (B) ACN containing 0.1% formic acid at a flow rate of 250 nL/min. Gradient was from 100% A to 60% B in 60 min. The effluent from the UPLC was infused directly into a Waters Q-ToF using a Waters nano-ESI ion source. Control and data acquisition was done using Waters MassLynx 4.1 (Milford, MA, USA), after an initial full scan, the top four most intense ions were subjected to MS/MS fragmentation by collision-induced dissociation. Data processed by Waters ProteinLynx Global Server (version 2.2.5) and by Mascot version 2.3 (Matrix Sciences, London, UK). The resulting sequence was searched against NCBI NR Protein database.

2.9 Fluorescence confocal microscopy of lunasin-treated THP-1 macrophages

Briefly, 9×10^4 THP-1 monocytes suspended in 300 μL phenol red-free RPMI-1640 medium and 10 ng/mL PMA were differentiated into macrophages for 48 h in an ibiTreat microscopy chamber (ibidi) at 37°C in 5% CO2/95% air. Cells were washed three times in fresh medium and treated with lunasin (1 μM) or echistatin (400 nM), an inhibitor of αVβ3, for 24 h. Cells were washed once with fresh medium, followed by three additional washes with PBS and fixed with 4% paraformaldehyde aqueous solution (Electron Microscopy Sciences) for 30 min at 25°C; washed three times (5 min each) with PBS, and permeabilized with 0.1% Triton X 100 in PBS for 15 min at 25°C. Cells were washed once with PBS and incubated with ultracold HPLC-grade methanol for 15 min at −20°C. Methanol was removed, replaced with PBS, and incubated at 25°C for 30 min. Cells were blocked with Image-iT FX Signal Enhancer (Life Technologies) for 30 min at 25°C, washed once with PBS, and incubated with lunasin polyclonal (1:500) and αVβ3 monoclonal antibodies (1:50) for 3 h at 25°C. Cells were washed three times (5 min each) with PBS and incubated with Alexa Fluor 568 Goat Anti-Rabbit IgG and Alexa Fluor 488 Goat Anti-Mouse IgG (Life Technologies) secondary antibodies (1:200) for 90 min at 25°C in the dark. Cells were washed three times (5 min each) with PBS and cured with ProLong Gold antifade reagent with DAPI (Life Technologies) for 24 h at 25°C in the dark. The microscopy chamber plate was stored at 4°C in the dark until analysis. The cells were visualized using Carl Zeiss LSM 700 Laser Scanning Microscope (Carl Zeiss AG, Germany) with 63× oil immersion objective. Total intensities and area sums (μm^2) were quantified with AxioVision Rel 4.8 (Carl Zeiss).

2.10 Statistical analysis

Data were analyzed using one-way analysis of variance (ANOVA) using Statistical Analysis System software version 9.3 (SAS Institute, Cary, NC, USA). Means of $n = 3$ were generated and adjusted with Least Significant Difference. Significant differences were reported at $p < 0.05$.

3 Results

3.1 Lunasin inhibited NF-κB-dependent markers of LPS-induced inflammation

Lunasin reduced exogenous NO secretion in a dose-dependent manner (Fig. 1A) and treatments at 10, 25, and 50 μM inhibited NO production by 65.9, 72.1, and 76.2%, respectively. Lunasin, at the same concentrations, reduced the expression of iNOS dose dependently, with expressions decreased by 27.2, 51.3, and 64.5%, respectively (Fig. 1B).

Protein expression of COX-2 was dose dependently inhibited by 15.9, 47.2, and 57.9%, respectively, following lunasin treatment at 10, 25, and 50 μM (Fig. 1C). Lunasin caused a dose-dependent reduction in the concentration of PGE_2. Treatments at the same concentrations resulted in a 74.1, 85.3, and 92.5% reduction in exogenous secretion of PGE_2 (Fig. 1D).

3.2 Lunasin inhibited Akt-mediated activation of NF-κB and reduced TNF-α in LPS-induced THP-1 macrophages

Treatment with lunasin resulted in a dose-dependent reduction in the activated forms of Akt and NF-κB subunit p65. Lunasin treatment at 10, 25, and 50 μM decreased the activation of p-Akt by 30.1, 44.7, and 59.5%, respectively (Fig. 2A). At the same concentrations, lunasin inhibited the activation of NF-κB p-p65 by 41.6, 60.1, and 74.5% (Fig. 2B).

Lunasin reduced the concentration of TNF-α in a dose-dependent manner. At 10, 25, and 50 μM, lunasin inhibited exogenous release of TNF-α by 21.9, 51.7, and 94.9%, respectively when compared to PBS control (Fig. 2C).

3.3 In combined LPS and vitronectin-induced THP-1 macrophages, lunasin attenuated production of NO and protein expressions of NF-κB p-p65 and p-Akt

Vitronectin (10 μg/mL) treatment alone increased markers of inflammation to a similar effect as LPS in THP-1 macrophages. Lunasin pretreatments (50 and 100 μM) for 2 h of THP-1 macrophages induced with vitronectin (10 μg/mL) alone resulted in a 47.6 and 73.5% reduction in

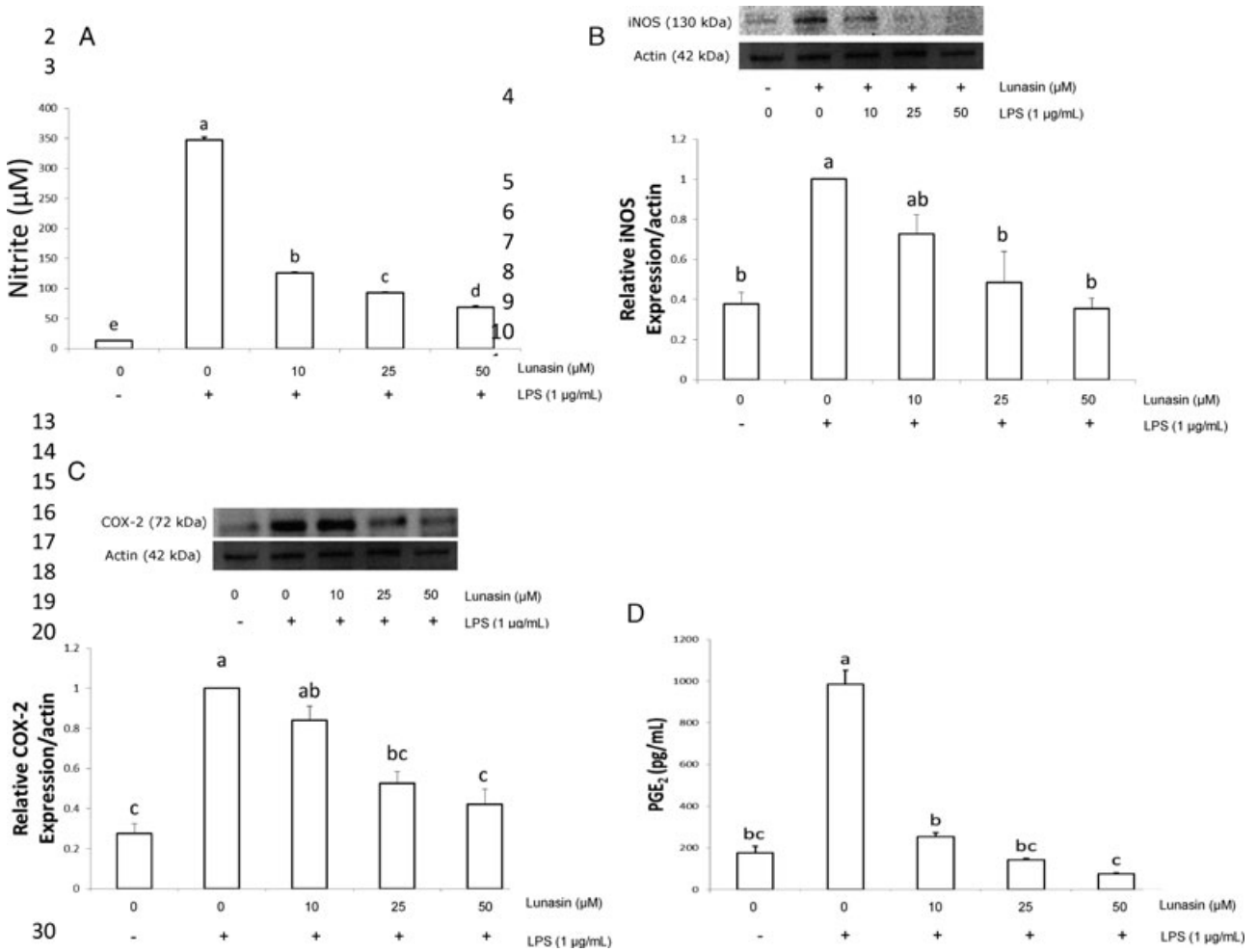

Figure 1. Lunasin inhibited the production of (A) NO and (B) iNOS in THP-1 macrophages at 10, 25, and 50 μM. Concentrations of NO were determined by conducting a colorimetric nitric oxide assay on the spent media. Lunasin inhibited (C) COX-2 and (D) PGE_2 in LPS-induced inflammation in THP-1 macrophages in a dose-dependent manner. Expressions of iNOS and COX-2 were performed by Western blot (20 μg protein/well). Means with different values are significantly different from each other ($n = 3$, $p < 0.05$).

NO production (Fig. 3A). Lunasin treatment at these same concentrations decreased phosphorylation of NF-κB p-p65 by 22.8 and 47.7%, respectively (Fig. 3B). However, lunasin did not modulate the expression of p-Akt in vitronectin-induced THP-1 macrophages (Fig. 3C).

Treatment of THP-1 macrophages with combined LPS and vitronectin (10 μg/mL), αVβ3 integrin ligand, increased NO production and phosphorylation of NF-κB p-p65 and p-Akt by 50.6, 65.1, and 31.5%, respectively, compared to vitronectin alone (Fig. 3A–C). Pretreatment with lunasin (50 and 100 μM) inhibited combined LPS- and vitronectin-induced upregulation of NO by 72.7 and 84.8%, respectively (Fig. 3A). Lunasin (50 and 100 μM) pretreatment of cells stimulated with LPS-vitronectin, reduced phosphorylation of NF-κB p-p65 by 40.6 and 38.4%, respectively (Fig. 3B). At these same concentrations, lunasin reduced phosphorylation of p-Akt by 51.4 and 60.7%, respectively (Fig. 3C).

3.4 Lunasin interacted with αVβ3 integrin receptor in THP-1 macrophages, confirmed by LC/MS/MS.

Co-immunoprecipitation of αVβ3 integrin cell membrane receptor in lunasin-treated (10 μM) THP-1 macrophages confirmed direct interaction with lunasin. There was no observed interaction with the Co-IP pull down of normal IgG and untreated cells, whereas the lunasin-treated cells reacted positively with lunasin antibody (Fig. 4B). Subsequent LC/MS/MS analysis of the in-gel tryptic digest of lunasin obtained from the lunasin/αVβ3 integrin complex detected the complete 43 amino acid sequence of lunasin (Fig. 4C). Additionally, fragmentation of one of the lunasin peptide segments, HIMEKIQGRGDDDDDD, yielded an ions score of 60, indicating that the Co-IP lunasin sequence and its corresponding spectra matched significantly with the lunasin

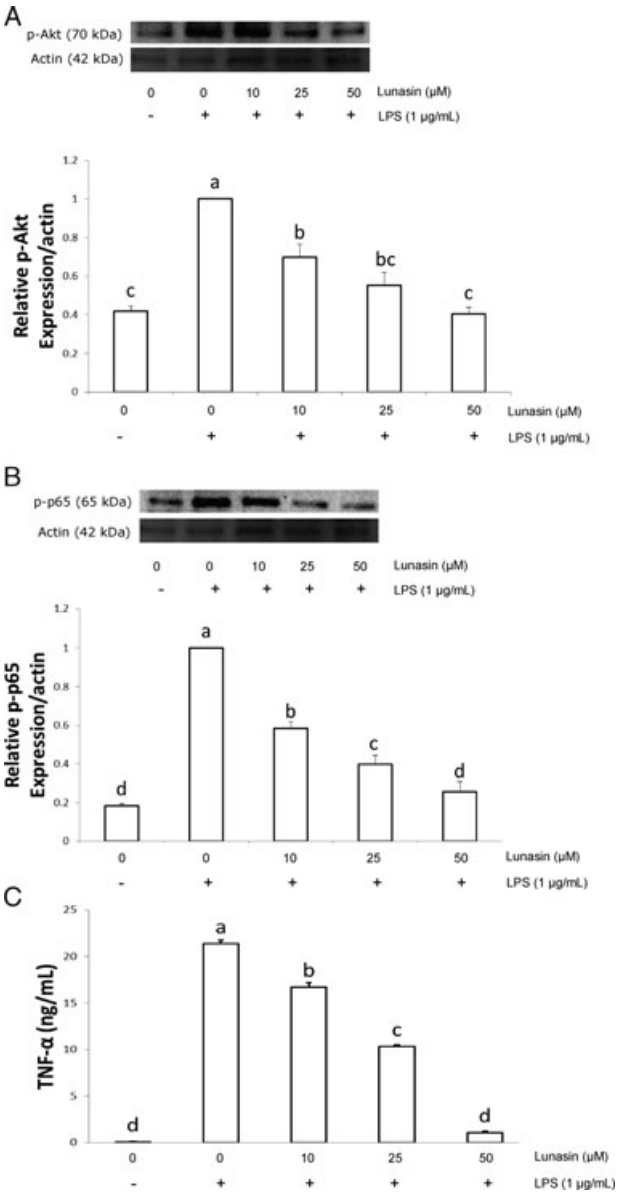

Figure 2. Lunasin inhibited the activation of (A) p-Akt and (B) NF-κB p-p65 in a dose-dependent manner in THP-1 macrophages. (C) Lunasin reduced the production of TNF-α in the spent medium of THP-1 macrophages. Means with different values are significantly different from each other ($n = 3$, $p < 0.05$).

sequence in the *Glycine max* (soybean) database (Fig. 4D and E). Individual ions scores >50 indicate identity or extensive homology.

3.5 Lunasin internalized into macrophages within intracellular vesicles and modulated αVβ3 integrin expression

Lunasin was rapidly recruited within intracellular vesicles integrated in a punctate pattern (Fig. 5A and B), compared to the quiescent PBS control (Fig. 5C). Additionally, at 30 min and 24 h, accumulation of lunasin punctate at specific intracellular regions concurrently reduced αVβ3 integrin expression at the cellular membrane in those respective areas (Fig. 5D and E). In contrast, PBS control did not have an observed effect on αVβ3 integrin expression and remained constitutively expressed (Fig. 5F). In the merged images at 30 min and 24 h, heterogeneous uptake of lunasin (Fig. 5J and K) showed sites of cells with high aggregations of lunasin punctate corresponded with a reduction in αVβ3 integrin expression (open arrowhead), whereas specific areas of cells with low concentrations of lunasin punctate (solid arrowhead) maintained their respective integrin expression.

3.6 Intracellular accumulation of lunasin reduced total αVβ3 integrin intensity, whereas αVβ3 integrin inhibitor, echistatin, attenuated lunasin uptake into macrophages

Immunofluorescence of 2-D median optical planes of lunasin-treated (1 μM) macrophages showed total lunasin intensity (solid arrowhead) increased rapidly over time and reached its plateau at 24 h (Fig. 6A–D). Compared to PBS control (Fig. 6E), total lunasin intensities at 30 sec, 15 min, and 24 h increased by 8.6-, 19.2-, and 22.3-fold, respectively. As treatment time progressed, lunasin intensity was amplified, while total αVβ3 integrin intensity (open arrowhead) at the cell membrane surface decreased (Fig. 6F–H). Total αVβ3 integrin intensities decreased by 6.8-, 4.5-, and 1.7-fold at 30 sec, 15 min, and 24 h of lunasin treatment, respectively. In the merged images, compared to PBS control (Fig. 6M), as total lunasin intensity increased significantly in conjunction with accumulation of lunasin punctate, there was a marked reduction in total αVβ3 integrin intensity at the cellular membrane (Fig. 6N–P). Pretreatment with αVβ3 inhibitor, echistatin (400 nM), followed by lunasin (1 μM) for 24 h decreased total lunasin intensity (oval arrowhead) and reduced the prevalence of lunasin punctate, compared to lunasin treatment alone (Fig. 6Q–T). Quantification of total intensities showed that while lunasin treatment modulated integrin expression and lunasin uptake was reduced by the presence of echistatin, αVβ3 integrin intensity (diamond arrowhead, Fig. 6R) was not significantly affected in macrophages pretreated first with the αVβ3 integrin inhibitor (Fig. 6U).

4 Discussion

The prevention of macrophage entry into a chronic proinflammatory state is crucial in reducing the prevalence of vascular diseases such as CVD [27]. The αVβ3 integrin (vitronectin receptor, CD51/CD61) mediates signaling cascades between the extracellular matrix and intracellular medium, and binds proteins and peptides with RGD motifs [28]. The expression of this specific integrin is highly upregulated in cells in pathogenic tissues such as atherosclerotic lesions [29]. In this study, we present data on the role of lunasin

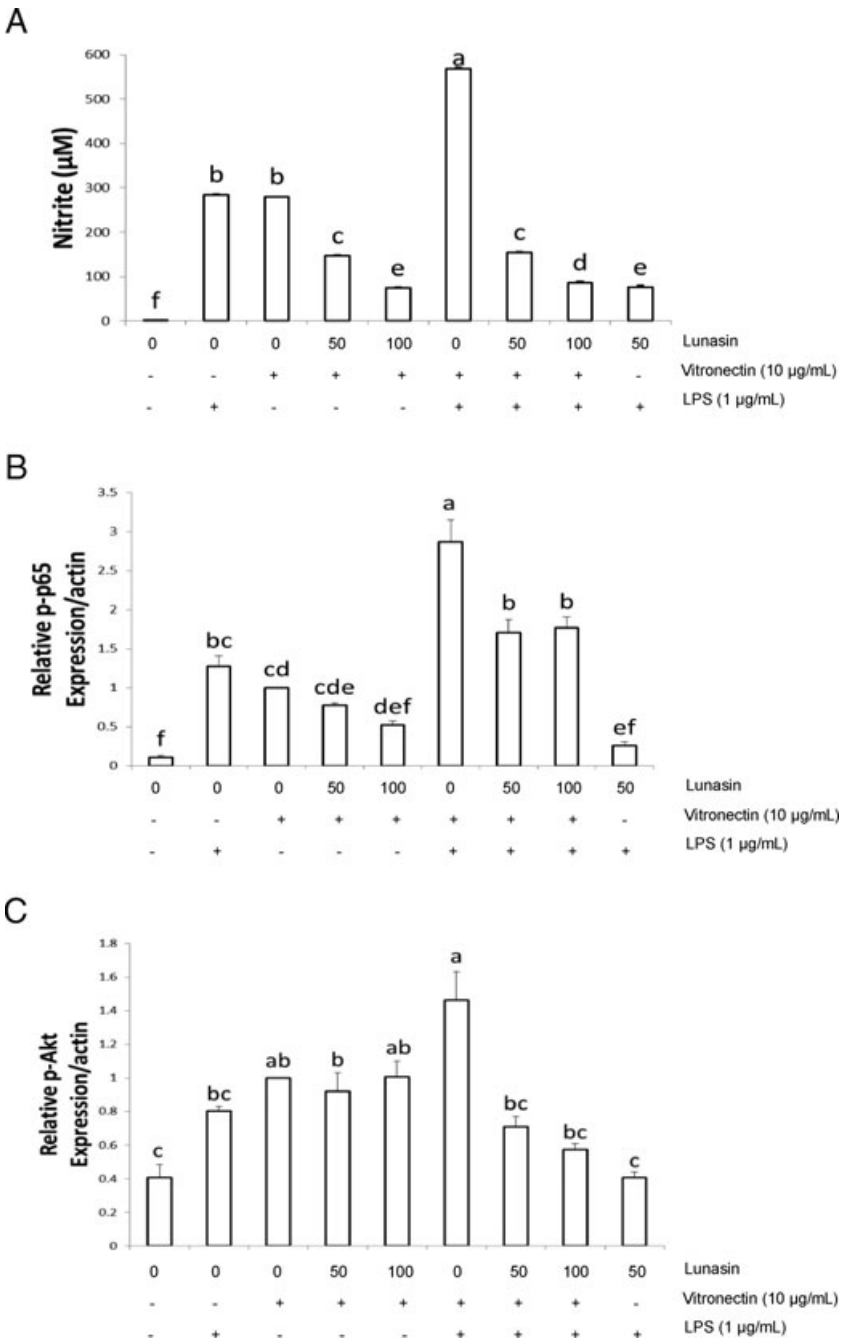

Figure 3. (A) Lunasin inhibited the production of NO in LPS and vitronectin-induced THP-1 macrophages. Concentrations of NO were determined by conducting a colorimetric nitric oxide assay on the spent media. (B) Lunasin reduced phosphorylation of NF-κB p-p65 in LPS and vitronectin-induced THP-1 macrophages. (C) Lunasin reduced phosphorylation of p-Akt in LPS and vitronectin-induced THP-1 macrophages. Lunasin did not modulate p-Akt expression in the presence of vitronectin alone (without LPS). Means with different values are significantly different from each other ($n = 3$, $p < 0.05$).

in the inhibition of Akt-mediated NF-κB activation though interaction with αVβ3 integrin receptor in human THP-1 macrophages.

Lunasin downregulated LPS-induced phosphorylation of Akt and NF-κB subunit p65 in human THP-1 macrophages by potentially inhibiting the activation of αVβ3 integrin. Extracellular growth factors and cytokines upregulate PI3K activity, resulting in Akt activation and translocation into the nucleus where it functions to activate downstream signaling pathways [30, 31]. Silencing the αV integrin subunit with siRNA inhibited LPS-induced IL-6 and TNF-α release compared to the negative control in THP-1 macrophages [32], further suggesting αVβ3 integrin is critically involved in mediating the activation of key regulators of inflammation. Other bioactive compounds have also been reported to inhibit Akt activation and subsequently downregulate NF-κB in LPS-stimulated U937 macrophages [33]. These prior data suggest that the αVβ3 integrin is an important receptor to target as a measure to resolve inflammation and prevent the progression of atherosclerosis.

A

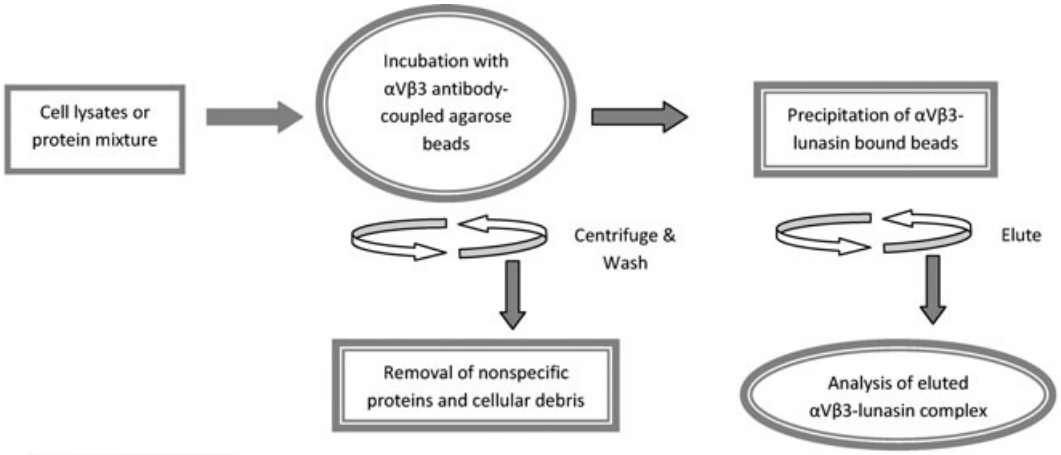

B

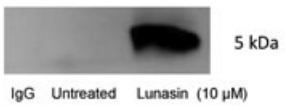

C

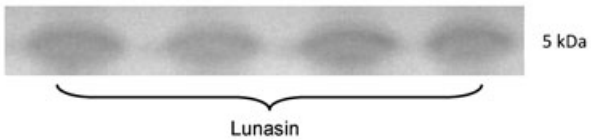

Lunasin sequence: SKWQHQQDSCRKQLQGVNLTPCEKHIMEKIQGRGDDDDDDDDD

D

Monoisotopic Mass	Ions Score	Sequence
1104.4200	28	IQGRGDDDDD
1219.4442	39	IQGRGDDDDDD
1334.4678	47	IQGRGDDDDDDD
1528.6690	30	HIMEKIQGRGDDD
1564.5154	59	IQGRGDDDDDDDDD
1758.7369	18	HIMEKIQGRGDDDDD
1873.7434	60	HIMEKIQGRGDDDDDD
2202.8194	26	HIMEKIQGRGDDDDDDDDD
2218.8172	39	HIMEKIQGRGDDDDDDDDD
3494.5881	6	SKWQHQQDSCRKQLQGVNLTPCEKHIMEK

E

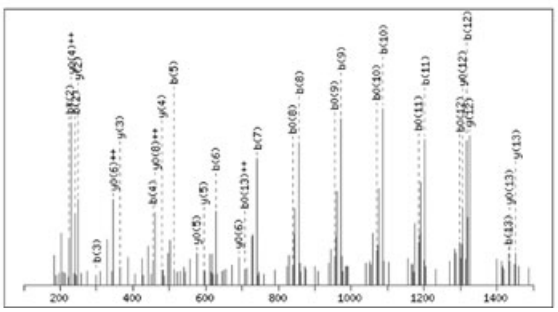

Figure 4. Lunasin directly interacted with the αVβ3 integrin receptor. THP-1 macrophages were treated with 10 μM lunasin for 24 h and harvested with RIPA buffer. (A) Schematic of the Co-IP assay. (B) Co-IP of the lunasin-αVβ3 integrin complex was performed with αVβ3 mAb ($n = 3$). C) LC/MS-MS results were determined with the in-gel tryptic digest of lunasin pulled down with Co-IP detected the entire 43-amino-acid lunasin sequence. (D) Sequences of the peptides within the in-gel tryptic digest of the band that matched with the 5-kDa lunasin sequence, their respective monoisotopic masses and ions scores. (E) Major sequences of lunasin were detected by MS/MS fragmentation and the corresponding spectra matched significantly with the lunasin sequence or its precursor 2S soy albumin.

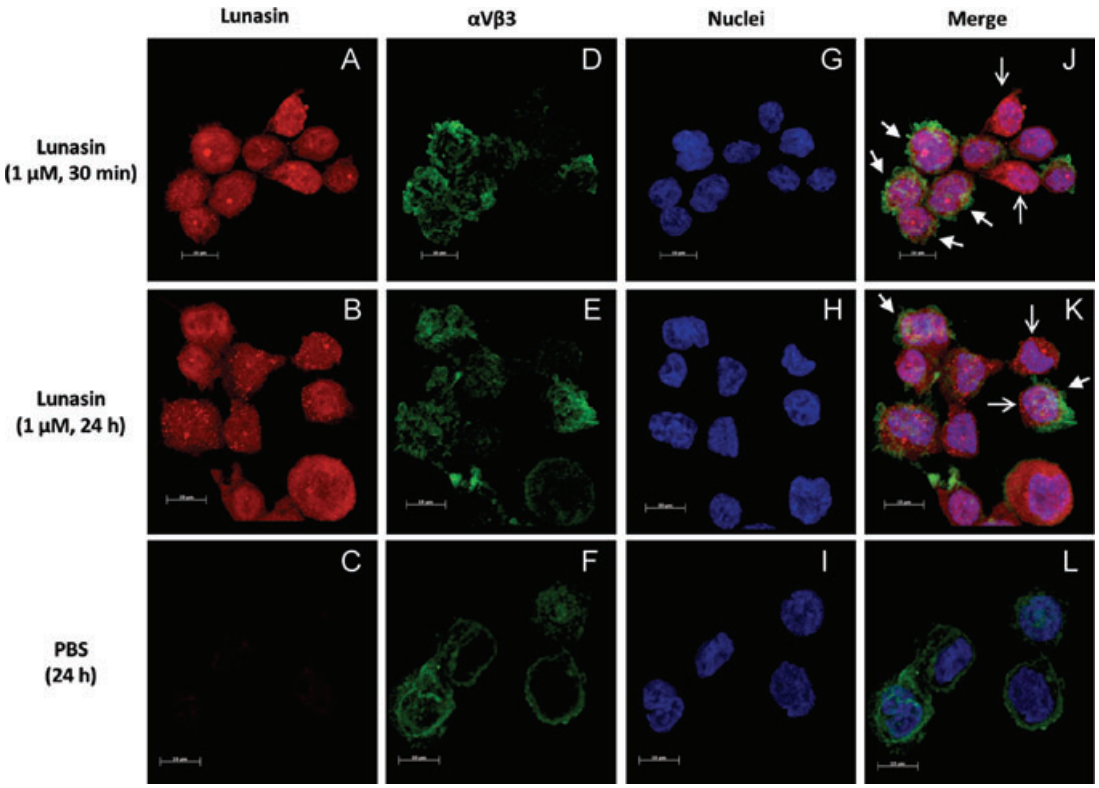

Figure 5. Confocal laser scanning microscopy depicting three-dimensional immunocytochemical localization of lunasin (red), αVβ3 integrin (green), and nuclei (blue) in human THP-1 macrophages after 30 min and 24 h lunasin treatment. (A, B) Recruitment of lunasin within intracellular vesicles localized into a punctate pattern, compared to the (C) quiescent PBS control. (D, E) αVβ3 integrin intensity was modulated at specific sites within the cell containing lunasin punctate. (F) αVβ3 integrin is constitutively expressed with PBS control in human THP-1 macrophages. (G–I) Nuclear staining. (J, K) Merge showing increased uptake of lunasin within intracellular sites corresponded with a reduction in αVβ3 integrin intensity (open arrowhead), whereas specific areas of cells without lunasin punctate maintained integrin intensities (solid arrowhead). (L) Merge of PBS control showing αVβ3 integrin intensity remained ubiquitously dispersed on the cell membrane. Images were taken at four independent fields per well for three independent replicates of cells. Scale = 10 μm.

Lunasin significantly inhibited NO and its respective protein, iNOS, markers which play an important role in regulating arterial wall integrity and endothelial function [34,35]. Under normal conditions, iNOS expression in vascular tissue is virtually quiescent, but upregulated in advanced atherosclerosis [36,37]. In rodents, decreases in iNOS correlated with a reduction in the development of atherosclerotic lesions [38,39]. In this study, lunasin, particularly at 50 μM, inhibited the COX-2/PGE_2 pathway, thereby preventing the biosynthesis of prostaglandins. Prostaglandins are attributed the progression of atherosclerotic lesions by maintaining macrophages in an active state through induction of chemotaxis, stimulation of smooth muscle cell migration, and activation of inflammatory cytokines [40].

In RAW 264.7 murine cells, lunasin (10 μM) inhibited NO and PGE_2 production by 43 and 13%, respectively [6]. In contrast, this study found that the same concentration reduced NO and PGE_2 by 65.9 and 74% in human THP-1 macrophages. These data suggest that THP-1 human macrophages are potentially more sensitive to lunasin treatment compared to murine macrophages, an effect consistent with prior data showing THP-1 cells as more responsive to particular compounds or nutrients, compared to epithelial or epidermal cells [41,42].

In this study, lunasin effectively inhibited the production of TNF-α, nearly abolishing its release at 50 μM concentrations. TNF-α is responsible for the regulation of macrophage activity after trauma, infection, or exposure to bacterial endotoxins such as LPS [43]. TNF-α upregulates adhesion molecules in monocytes and scavenger receptors in macrophages, leading to foam cell formation [44]. TNF-α and a member of the TNF cytokine superfamily, TNF-like protein 1A, were found to play a significant role in the promotion of macrophage foam cell formation and atherosclerosis by increasing the uptake of oxidized LDL [45]. Further, it has been reported that αVβ3 integrin expression mediates ERK activation, cell attachment, and the production of TNF-α in human THP-1 macrophages [46]. Blockade of the αVβ3 integrin by a specific antibody resulted in decreased cell adhesion and inhibition of TNF-α production. Treatment with synthetic lunasin (200 μM) in LPS-induced RAW 264.7 murine macrophages resulted in a 23% reduction in TNF-α [47]. In contrast, lunasin

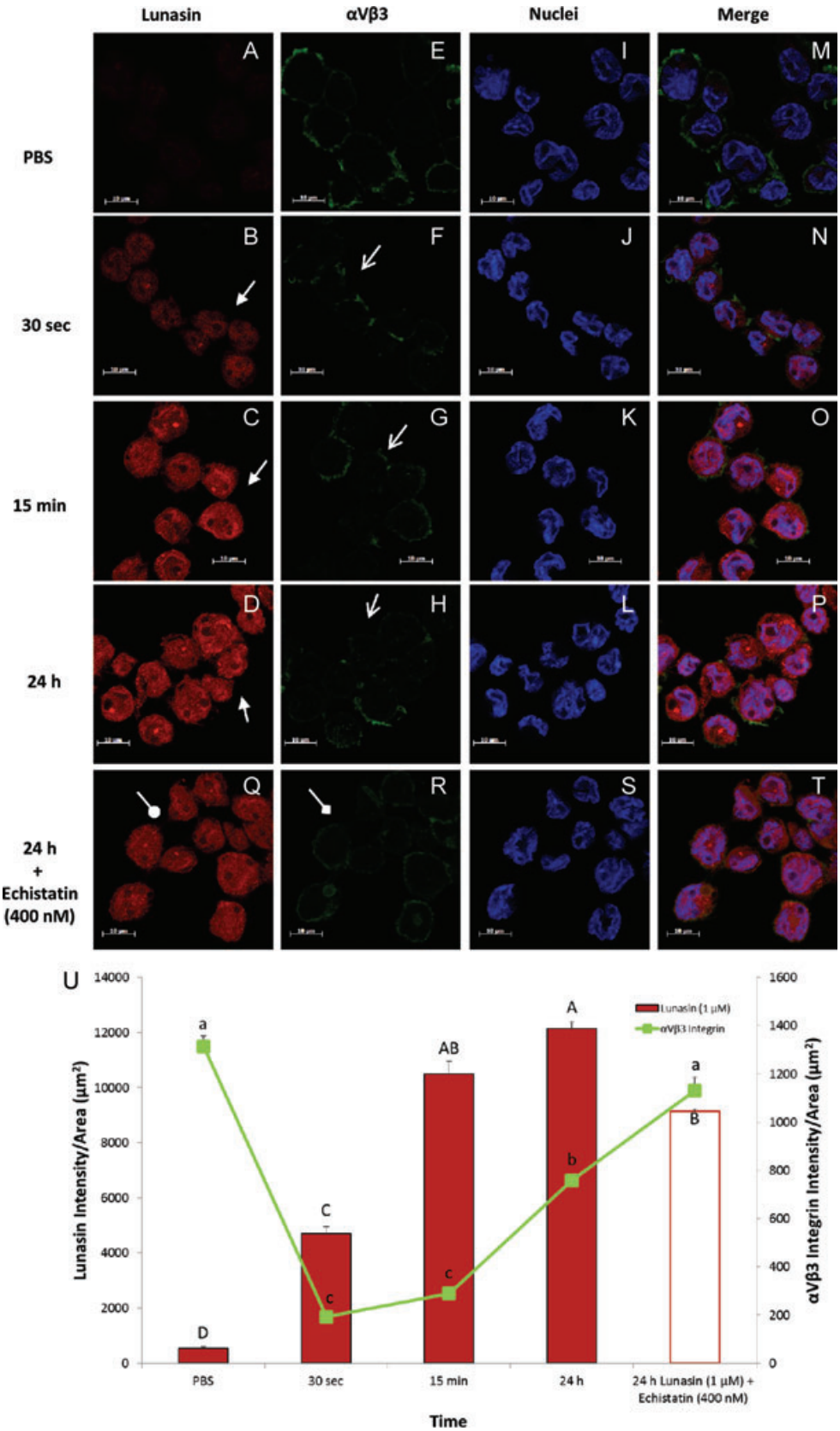

Figure 6. Immunofluorescence of 2-D median optical planes of lunasin-treated (1 μM) macrophages in chronological order. (A–D) Lunasin treatment (1 μM) increased total lunasin intensity (solid arrowhead), while (E–H) decreasing total αVβ3 intensity (open arrowhead) over time in human THP-1 macrophages. (I–L) Nuclear staining. (M–P) Merge depiction showing increased lunasin intensity with concomitant reduction in αVβ3 intensity at the cell membrane surface over time. (Q–T) Pretreatment with αVβ3 inhibitor, echistatin (400 nM), followed by lunasin (1 μM) for 24-h reduced total lunasin intensity (oval arrowhead) compared to lunasin treatment alone. Lunasin did not significantly affect αVβ3 intensity (diamond arrowhead) in cells pretreated with echistatin. (U) Quantification of total lunasin and αVβ3 intensity over their respective area sums over treatment time (μm^2). Means with different letters are significantly different from each other ($n = 2$, $p < 0.05$).

(10 μM) was sufficient to inhibit TNF-α by 21.8% in human THP-1 macrophages in this study. This difference in lunasin concentration may be attributed to cell lines, and variability in secondary folding structure of the synthetic lunasin and its ability to interact to the αVβ3 integrin receptor.

Although the effect of THP-1 macrophages induced with LPS was highly amplified when combined with vitronectin, lunasin attenuated the enhanced activation of proinflammatory markers, demonstrating its protective capacity in the presence of two potent agonists. Pathogen-associated molecular patterns from bacteria such as LPS stimulate Toll-like receptors (TLRs) and facilitate the differentiation of oxidized LDL-induced macrophages into foam cells and upregulate the production of proinflammatory markers in monocytes from patients with metabolic syndrome [48, 49]. Additionally, the activation of TLR2 and TLR4 by Pam(3)CSK(4) or LPS, respectively, elicited an enhanced inflammatory response through induction of CD11b on circulating monocytes and increased levels of TNF-α [50]. Vitronectin, a 75 kDa endogenous glycoprotein ligand, contains an RGD motif, activates αVβ3 integrins and has been found in atheroma [51, 52]. RGD peptides aimed at competing for αVβ3 integrin binding reduced neointima hyperplasia in animal models [53, 54]. In this study, lunasin significantly reduced NO production and NF-κB p-p65 and p-Akt in THP-1 macrophages induced with both vitronectin and LPS, suggesting its efficacy may be attributed through αVβ3 integrin blockade. Lunasin has the potential to prevent Akt-mediated activation of NF-κB p-p65 by diminishing extracellular binding of αVβ3 integrin with endogenous ligands such as vitronectin.

Lunasin physically interacted with αVβ3 integrin, substantiating the hypothesis that its biological activity is attributed to its antagonistic effect on αVβ3 receptors. Crystal structure of the extracellular segment of αVβ3 integrin in complex with an RGD ligand found binding interactions similar to that of echistatin, a RGD peptide with a molecular weight comparable to lunasin (5 kDa) [55]. The results suggest that lunasin possesses an affinity for αVβ3 in macrophages and prevents the activation of integrin-mediated inflammatory cascades by direct blockade. Food-derived peptides containing RGD motifs, such as lunasin, may have potentially similar effects.

Lunasin internalized into macrophages within intracellular vesicles and modulated αVβ3 integrin expression at the cell membrane surface, potentially through integrin-dependent pathways. The endocytosis of integrins and their respective ligands, such as RGD proteins or peptides, occurs primarily through clathrin-dependent or clathrin-independent endocytic mechanisms [15, 56]. A multimeric RGD peptide mediated αVβ3 integrin internalization and reduced the quantity of αVβ3 integrin at the cell surface by 79% versus the control via clathrin-dependent endocytosis in HEK293(β_3) cells [57]. Additionally, a mAb directed to αV was internalized by an integrin-dependent endocytic mechanism and reduced the number of functional integrin receptors at the cell surface in melanoma cells [58]. In the present study, total lunasin intensity and prevalence of intracellular punctate rapidly increased over time, with concomitant reduction in αVβ3 intensity at the cell membrane surface at specific areas with high intracellular lunasin concentrations, potentially through clathrin-dependent endocytic pathways. At 24 h, the intensity of integrin began to decrease, an effect potentially attributed to the regulation of integrin turnover by endocytosis and recycling over time.

Pretreatment of THP-1 macrophages with αVβ3 integrin inhibitor, echistatin, reduced total lunasin intensity and prevalence of punctate, further suggesting the potential for lunasin to internalize through an αVβ3 integrin-mediated pathway. Echistatin, a 49-amino-acid peptide derived from snake venom, is a high-affinity inhibitor of the αVβ3 integrin receptor and binds in a gradual, but nondissociable manner [59]. The binding of echistatin can be outcompeted by other RGD peptides and as a result, the observed reduction in lunasin intensity is potentially attributed to partial blockade of αVβ3 receptor by echistatin. The intensity of integrin αVβ3 was not significantly affected, possibly due to the fact that the capability of lunasin to bind and enter the cell was hindered by ligand occupancy and conformational modifications of the αVβ3 receptor by pretreatment with echistatin.

In summary, the results reported in this study demonstrate the potential of lunasin to inhibit αVβ3 integrin-mediated proinflammatory markers by downregulating the activation of Akt-mediated NF-κB pathways through interaction with αVβ3 integrin in THP-1 human macrophages. Lunasin may contribute at the molecular level in the prevention of CVD risk factors long associated with soy protein consumption.

Authors acknowledge Dr. Mayandi Sivaguru, Institute of Genomic Biology – Core Facilities, University of Illinois at Urbana-Champaign for assistance and training with confocal microscopy.

The authors have declared no conflict of interest.

5 References

[1] Heron, M. P., Hoyert, D. L., Murphy, S. L., Xu, J. Q. et al., Deaths: final data for 2006. National Vital Statistics Reports. *Natl. Vital Stat. Rep.* 2009, *57*, 1–134.

[2] Lloyd-Jones, D., Adams, R. J., Brown, T. M., Carnethon, M. et al., Executive summary: heart disease and stroke statistics–2010 update: a report from the American Heart Association. *Circulation* 2010, *121*, 948–954.

[3] Heidenreich, P. A., Trogdon, J. G., Khavjou, O. A., Butler, J. et al., Forecasting the future of cardiovascular disease in the United States. A policy statement from the American Heart Association. *Circulation* 2011, *123*, 933–944.

[4] Moore, K. J., Tabas, I., Macrophages in the pathogenesis of atherosclerosis. *Cell* 2011, *145*, 341–355.

[5] Dia, V. P., Berhow, M. A., De Mejia, E. G., Bowman-Birk inhibitor and genistein among soy compounds that synergistically inhibit nitric oxide and prostaglandin E(2) pathways

in lipopolysaccharide-induced macrophages. *J. Agric. Food Chem.* 2008, *56*, 11707–11717.

[6] de Mejia, E. G., Dia, V. P., Lunasin and lunasin-like peptides inhibit inflammation through suppression of NF-kappaB pathway in the macrophage. *Peptides* 2009, *30*, 2388–2398.

[7] Martinez-Villaluenga, C., Dia, V. P., Berhow, M., Bringe, N. A., de Mejia, E. G., Protein hydrolysates from β-conglycinin enriched soybean genotypes inhibit lipid accumulation and inflammation in vitro. *Mol. Nutr. Food Res.* 2009, *53*, 1007–1018.

[8] Food labeling: health claims; soy protein and coronary heart disease. Food and Drug Administration, HHS. Final rule. *Fed. Regist.* 1999, *64*, 57700–57733.

[9] Anderson, J. W., Bush, H. M., Soy protein effects on serum lipoproteins: a quality assessment and meta-analysis of randomized, controlled studies. *J. Am. Coll. Nutr.* 2011, *30*, 79–91.

[10] Tabas, I. Macrophage death and defective inflammation resolution in atherosclerosis. *Nat. Rev. Immunol.* 2010, *10*, 36–46.

[11] Dia, V. P., de Mejia, E. G., Lunasin induces apoptosis and modifies the expression of genes associated with extracellular matrix and cell adhesion in human metastatic colon cancer cells. *Mol. Nutr. Food Res.* 2011, *55*, 623–634.

[12] Dia, V. P., Torres, S., de Lumen, B. O., Erdman, J. W., Jr, de Mejia, E. G., Presence of lunasin in plasma of men after soy protein consumption. *J. Agric. Food Chem.* 2009, *57*, 1260–1266.

[13] Campbell, I. D., Humphries, M. J., Integrin structure, activation, and interactions. *Cold Spring Harb. Perspect. Biol.* 2011, *3*, a004994.

[14] Springer, T. A., Dustin, M. L., Integrin inside-out signaling and the immunological synapse. *Curr. Opin. Cell Biol.* 2012, *24*, 107–115.

[15] Kim, C., Ye, F., Ginsberg, M. H., Regulation of integrin activation. *Annu. Rev. Cell Dev. Biol.* 2011, *27*, 321–345.

[16] Kuphal, S., Bauer, R., Bosserhoff, A. K., Integrin signaling in malignant melanoma. *Cancer Metastasis Rev.* 2005, *24*, 195–222.

[17] Tan, T. W., Yang, W. H., Lin, Y. T., Hsu, S. F. et al., Cyr61 increases migration and MMP-13 expression via alphavbeta3 integrin, FAK, ERK and AP-1-dependent pathway in human chondrosarcoma cells. *Carcinogenesis* 2009, *30*, 258–268.

[18] Marsh, N., Williams, V., Practical applications of snake venom toxins in haemostasis. *Toxicon* 2005, *45*, 1171–1181.

[19] Furundzija, V., Fritzsche, J., Kaufmann, J., Meyborg, H. et al., IGF-1 increases macrophage motility via PKC/p38-dependent alphavbeta3-integrin inside-out signaling. *Biochem. Biophys. Res. Commun.* 2010, *394*, 786–791.

[20] Kitagawa, T., Kosuge, H., Uchida, M., Dua, M. M. et al., RGD-conjugated human ferritin nanoparticles for imaging vascular inflammation and angiogenesis in experimental carotid and aortic disease. *Mol. Imaging Biol.* 2011, *3*, 315–324.

[21] Antonov, A. S., Antonova, G. N., Munn, D. H., Mivechi, N. et al., Alpha V beta 3 Integrin regulates macrophage inflammatory responses via PI3 Kinase/Akt-dependent NF-kappa B activation. *J. Cell. Physiol.* 2011, *226*, 469–476.

[22] Nichols, T. C., du Laney, T., Zheng, B., Bellinger, D. A. et al., Reduction in atherosclerotic lesion size in pigs by alphaV-beta3 inhibitors is associated with inhibition of insulin-like growth factor-I-mediated signaling. *Circ. Res.* 1999, *85*, 1040–1045.

[23] Maile, L. A., Busby, W. H., Nichols, T. C., Bellinger, D. A. et al., A monoclonal antibody against alphaVbeta3 integrin inhibits development of atherosclerotic lesions in diabetic pigs. *Sci. Transl. Med.* 2010, *2*, 18ra11.

[24] Lee, C., Huang, C., Chen, M., Lin, C. et al., IL-8 increases integrin expression and cell motility in human chondrosarcoma cells. *J. Cell. Biochem.* 2011, *112*, 2549–2557.

[25] Dia, V. P., Wang, W., Oh, V. L., de Lumen, B. O., de Mejia, E. G., Isolation, purification and characterisation of lunasin from defatted soybean flour and in vitro evaluation of its anti-inflammatory activity. *Food Chem.* 2009, *114*, 108–115.

[26] Green, L., Wagner, D., Glogowski, J., Skipper, P. et al., Analysis of nitrate, nitrite, and [N-15]-labeled nitrate in biological fluids. *Anal. Biochem.* 1982, *126*, 131–138.

[27] Libby, P., Okamoto, Y., Rocha, V. Z., Folco, E., Inflammation in atherosclerosis: transition from theory to practice. *Circ. J.* 2010, *74*, 213–220.

[28] Aguzzi, M. S., Fortugno, P., Giampietri, C., Ragone, G. et al., Intracellular targets of RGDS peptide in melanoma cells. *Mol. Cancer* 2010, *9*, 84.

[29] Laitinen, I., Saraste, A., Weidl, E., Poethko, T. et al., Evaluation of alphavbeta3 integrin-targeted positron emission tomography tracer 18F-galacto-RGD for imaging of vascular inflammation in atherosclerotic mice. *Circ. Cardiovasc. Imaging* 2009, *2*, 331–338.

[30] Calleja, V., Alcor, D., Laguerre, M., Park, J. et al., Intramolecular and intermolecular interactions of protein kinase B define its activation in vivo RID E-7465–2010. *PLoS Biol.* 2007, *5*, 780–791.

[31] Hers, I., Vincent, E. E., Tavare, J. M., Akt signalling in health and disease. *Cell Signal.* 2011, *23*, 1515–1527.

[32] Hsu, C. C., Chuang, W. J., Chang, C. H., Tseng, Y. L. et al., Improvements in endotoxemic syndromes using a disintegrin, rhodostomin, through integrin alpha v beta 3-dependent pathway. *J. Thromb. Haemost.* 2011, *9*, 593–602.

[33] Yasuda, T., Hyaluronan inhibits Akt, leading to nuclear factor-kappa B down-regulation in lipopolysaccharide-stimulated U937 macrophages. *J. Pharmacol. Sci.* 2011, *115*, 509–515.

[34] Foerstermann, U., Oxidative stress in vascular disease: causes, defense mechanisms and potential therapies. *Nat. Clin. Pract. Cardiovasc. Med.* 2008, *5*, 338–349.

[35] Forstermann, U., Nitric oxide and oxidative stress in vascular disease. *Pflugers Arch.* 2010, *459*, 923–939.

[36] Behr-Roussel, D., Rupin, A., Sansilvestri-Morel, P., Fabiani, J. et al., Histochemical evidence for inducible nitric oxide synthase in advanced but non-ruptured human atherosclerotic carotid arteries. *Histochem. J.* 2000, *32*, 41–51.

[37] Terashima, M., Ehara, S., Yang, E., Kosuge, H. et al., In vivo bioluminescence imaging of inducible nitric oxide synthase

gene expression in vascular inflammation. *Mol. Imaging Biol.* 2011, *13*, 1061–1066.

[38] Detmers, P., Hernandez, M., Mudgett, J., Hassing, H. et al., Deficiency in inducible nitric oxide synthase results in reduced atherosclerosis in apolipoprotein E-deficient mice RID D-2074–2010. *J. Immunol.* 2000, *165*, 3430–3435.

[39] Hayashi, T., Matsui-Hirai, H., Fukatsu, A., Surni, D. et al., Selective iNOS inhibitor, ONO1714 successfully retards the development of high cholesterol diet-induced atherosclerosis by novel mechanism. *Atherosclerosis* 2006, *187*, 316–324.

[40] Pistoia, F., Cipollone, F., Ferri, C., Sara, M. et al., Cyclooxygenase and atherosclerosis: a smoking area. *Curr. Pharm. Des.* 2010, *16*, 2567–2571.

[41] Jeffes, E., McCullough, J., Pittelkow, M., McCormick, A. et al., Methotrexate therapy of psoriasis—differential sensitivity of proliferating lymphoid and epithelial-cells to the cytotoxic and growth-inhibitory effects of methotrexate. *J. Invest. Dermatol.* 1995, *104*, 183–188.

[42] Fedorov, S. N., Makarieva, T. N., Guzii, A. G., Shubina, L. K. et al., Marine two-headed sphingolipid-like compound Rhizochalin inhibits EGF-induced transformation of JB6 P(+) Cl41 cells. *Lipids* 2009, *44*, 777–785.

[43] Parameswaran, N., Patial, S., Tumor necrosis factor-alpha signaling in macrophages. *Crit. Rev. Eukaryot. Gene Expr.* 2010, *20*, 87–103.

[44] Hsu, H., Twu, Y., Tumor necrosis factor-alpha-mediated protein kinases in regulation of scavenger receptor and foam cell formation on macrophage. *J. Biol. Chem.* 2000, *275*, 41035–41048.

[45] McLaren, J.E., Calder, C. J., McSharry, B.P., Sexton, K. et al., The TNF-like protein 1A-death receptor 3 pathway promotes macrophage foam cell formation in vitro. *J. Immunol.* 2010, *184*, 5827–5834.

[46] Kurihara, Y., Nakahara, T., Furue, M., Alpha V beta 3-integrin expression through ERK activation mediates cell attachment and is necessary for production of tumor necrosis factor alpha in monocytic THP-1 cells stimulated by phorbol myristate acetate. *Cell. Immunol.* 2011, *270*, 25–31.

[47] Hernandez-Ledesma, B., Hsieh, C., de Lumen, B. O., Antioxidant and anti-inflammatory properties of cancer preventive peptide lunasin in RAW 264.7 macrophages. *Biochem. Biophys. Res. Commun.* 2009, *390*, 803–808.

[48] Howell, K. W., Meng, X., Fullerton, D. A., Jin, C. et al., Toll-like receptor 4 mediates oxidized LDL-induced macrophage differentiation to foam cells. *J. Surg. Res.* 2011, *171*, E27–E31.

[49] Jialal, I., Huet, B. A., Kaur, H., Chien, A., Devaraj, S., Increased toll-like receptor activity in patients with metabolic syndrome. *Diabetes Care* 2012, *35*, 900–904.

[50] Scholtes, V. P. W., Versteeg, D., de Vriest, J. P. M., Hoefer, I. E. et al., Toll-like receptor 2 and 4 stimulation elicits an enhanced inflammatory response in human obese patients with atherosclerosis. *Clin. Sci.* 2011, *121*, 205–214.

[51] Dufourcq, P., Couffinhal, T., Alzieu, P., Daret, D. et al., Vitronectin is up-regulated after vascular injury and vitronectin blockade prevents neointima formation. *Cardiovasc. Res.* 2002, *53*, 952–962.

[52] Ekmekci, O., Ekmekci, H., Vitronectin in atherosclerotic disease. *Clin. Chim. Acta* 2006, *368*, 77–83.

[53] Choi, E., Engel, L., Callow, A., Sun, S. et al., Inhibition of neointimal hyperplasia by blocking alpha(v)beta(3), integrin with a small peptide antagonist Gpengrgdspca. *J. Vasc. Surg.* 1994, *19*, 125–134.

[54] Srivatsa, S., Fitzpatrick, L., Tsao, P., Reilly, T. et al., Selective alpha v beta 3 integrin blockade potently limits neointimal hyperplasia and lumen stenosis following deep coronary arterial stent injury: evidence for the functional importance of integrin alpha v beta 3 and osteopontin expression during neointima formation. *Cardiovasc. Res.* 1997, *36*, 408–428.

[55] Xiong, J., Stehle, T., Zhang, R., Joachimiak, A. et al., Crystal structure of the extracellular segment of integrin alpha V beta 3 in complex with an Arg-Gly-Asp ligand. *Science* 2002, *296*, 151–155.

[56] Margadant, C., Monsuur, H. N., Norman, J. C., Sonnenberg, A., Mechanisms of integrin activation and trafficking. *Curr. Opin. Cell Biol.* 2011, *23*, 607–614.

[57] Sancey, L., Garanger, E., Foillard, S., Schoehn, G. et al., Clustering and internalization of integrin alphavbeta3 with a tetrameric RGD-synthetic peptide. *Mol. Ther.* 2009, *17*, 837–843.

[58] Castel, S., Pagan, R., Mitjans, F., Piulats, J. et al., RGD peptides and monoclonal antibodies, antagonists of alpha(v)-integrin, enter the cells by independent endocytic pathways. *Lab. Invest.* 2001, *81*, 1615–1626.

[59] Szabo, A. M., Howell, N. R., Pellegrini, P., Greguric, I. et al., Development and validation of competition binding assays for affinity to the extracellular matrix receptors, alpha(v)beta(3) and alpha(IIb)beta(3) integrin. *Anal. Biochem.* 2012, *423*, 70–77.

